Engineering Structures 219 (2020) 110864

Contents lists available at ScienceDirect

Engineering Structures

journal homepage: www.elsevier.com/locate/engstruct

Optimal seismic retrofitting of reinforced concrete buildings by steel-jacketing using a genetic algorithm-based framework

Fabio Di Trapani[a,*], Marzia Malavisi[a], Giuseppe Carlo Marano[a], Antonio Pio Sberna[a], Rita Greco[b]

[a] Dipartimento di Ingegneria Strutturale, Edile e Geotecnica, Politecnico di Torino, Corso Duca degli Abruzzi 24, 10129 Turin, Italy
[b] Dipartimento di Ingegneria Civile, Ambientale, del Territorio, Edile e di Chimica, Politecnico di Bari, Italy

ARTICLE INFO

Keywords:
Steel jacketing
Retrofitting
Genetic algorithm
Pushover
Optimization

ABSTRACT

Retrofitting of existing reinforced concrete (RC) frame structures by steel angles and battens (steel-jacketing) is a commonly employed technique used to retrofit beams and columns against gravity and seismic loads. Steel-jacketing (SJ) effectively provides additional deformation and strength capacity to RC members but its application is associated with noticeable downtime of the building and non-negligible costs, depending on the amount of structural and non-structural manufacturing and materials. This paper presents an optimization framework aimed at the minimization of seismic retrofitting-related costs by an optimal placement (topological optimization) and amount of steel-jacketing reinforcement. In the proposed framework a 3D RC frame fiber-section model implemented in OpenSees is handled by a genetic algorithm routine that iterates reinforcement configurations to match the optimal solution. The feasibility of each solution is controlled by the outcomes of a static pushover analysis in the framework of N2 method. Results will provide optimized location and amount of steel-jacketing reinforcement, showing how effective and sustainable reduction of retrofitting costs is achievable maintaining a specified safety level.

1. Introduction

Retrofitting of reinforced concrete columns with cages arranged by steel angles and battens (steel jacketing) is a widely employed technique to improve strength and deformation capacity of beams and columns of existing buildings presenting critical conditions with respect to seismic and gravity loads. Steel jacketing of columns can be generally arranged in two ways. The first provides a moment resisting connection between the steel cages and the slabs (Fig. 1a). In this case, besides the confinement action exerted by the cage, additional flexural strength is provided. Since moment resisting connection are not always easy to realize, steel jacketing is often arranged by simply applying the cages (Fig. 1b). Even in this case, a certain additional flexural resistance is observed because of friction forces transfer between the steel angles and the concrete column (Campione et al. 2017 [1]), but the most significant contribution is related to the increase of deformation capacity as consequence of the strong confinement action. Experimental and numerical investigation have been carried out in the last years both for the first [2–5] and the second [1,6–10] typology of arrangement.

Despite its effectiveness in providing additional strength and deformation capacity to RC members, it should be said that steel jacketing is an invasive strengthening technique. In fact, the reinforcement of columns provides also the demolition and reconstitution of eventual portions of masonry infills and plaster. This is associated with significant direct costs and noticeable downtime for the building. A second issue regards the design of the intervention in terms of individuation of the columns to retrofit and the choice of the battens area and spacing. In fact, when approaching by non-linear static analysis (pushover), as a method to assess the performance before and after retrofitting intervention, a significant number of attempt iterations are needed to individuate the most suitable retrofitting configuration, especially when the number of columns is large and the building has irregular configuration. In the absence of a specific optimization process this generally brings the designer to adopt overall compromise solutions which allow obtaining effective seismic performance without optimization of the costs. Structural optimization is widely recognized as a valuable computational tool allowing engineers to obtain cost-effective designs. A number of seismic design optimization applications for steel and reinforced concrete structures (e.g. [11–16]) are presented in the literature. On the other hand, the issue of the optimization of strengthening and retrofitting interventions for reinforced concrete structural elements has not been investigated many times in the past and available studies are limited to the optimization of carbon fiber reinforcement of concrete slabs (Chaves and Cunha 2014 [17]) or FRP jackets (Chisari

* Corresponding author.
E-mail address: fabio.ditrapani@polito.it (F. Di Trapani).

https://doi.org/10.1016/j.engstruct.2020.110864
Received 14 November 2019; Received in revised form 16 April 2020; Accepted 25 May 2020

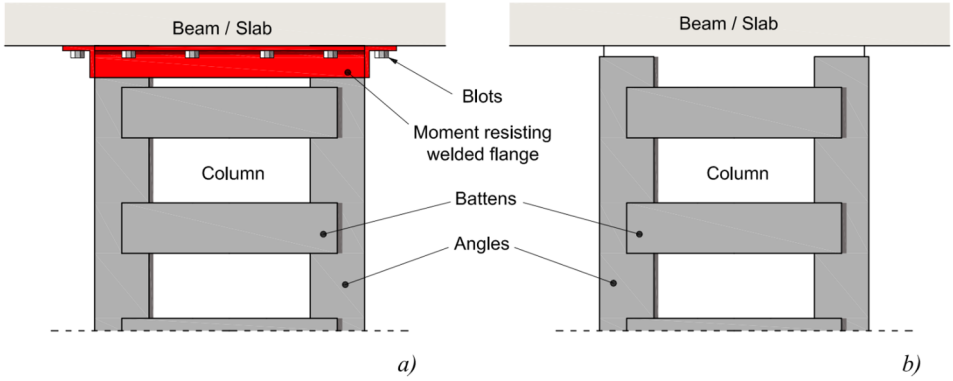

Fig. 1. Column steel-jacketing arrangements: (a) cage with moment resisting end connections; (b) cage without end connections.

and Bedon 2016 [18], Seo et al. 2018 [19]). More studies faced the optimization of fluid viscous dampers (Pollini et al. 2017 [20]), dissipative bracings (Braga et al. 2019 [21]) or both (Lavan and Dargush 2009 [22]) as retrofitting devices for frame buildings. In this context, it is noteworthy observing that, the very common steel-jacketing reinforcement technique has never been faced within an optimization framework, especially in consideration of the potentialities offered by artificial intelligence algorithms (Quaranta et al. 2020 [23]).

Based on the aforementioned premises, this paper presents a novel optimization framework operating on reinforced concrete buildings not designed to support seismic loads. The optimization framework is aimed at minimizing seismic retrofitting costs by determining the optimal configuration of the steel jacketing reinforcement of columns in terms of reinforcement location (topological optimization) and spacing between steel battens. Results are driven by the outcomes of the pushover assessment (N2 method, Fajfar 2000 [24]) in terms of feasibility of the solution obtained for the single generated individuals. The proposed procedure makes use of Matlab® genetic algorithm (GA) tool, automatically interfaced with the 3D model of the building realized in OpenSees (McKenna et al. 2000 [25]). The application of the methodology is shown for a case study RC building, showing how the capability of artificial intelligence algorithms (genetic algorithms) can be applied to seismic engineering problems in order to improve the sustainability and the effectiveness of retrofitting interventions.

2. Modelling of steel-jacketing action and application to RC fiber-section columns

As mentioned in the introduction, steel jacketing can be arranged to provide additional confinement only or additional flexural resistance besides confinement. Modelling of steel jacketing in fiber-section elements has been addressed by Campione et al (2017) [1] who provided that, for the case in which only confinement is considered, steel angles are not included in the cross-section assembly (Fig. 2a). On the contrary, in case of full flexural connection, also angels are discretized into fibers having specific uniaxial behaviour (Fig. 2b).

Focusing on confinement action, for both the ways of arrangement, this is introduced in retrofitted columns by simply modifying the stress–strain curve of concrete fibers (Fig. 2a, 2b). To determine the confined stress–strain response of concrete to assign to the core fibers, the approach by Montuori and Piluso (2009) [3] is here combined with the expressions provided by Razvi and Saatcioglu (1992) [26], so that peak (f_{cc},ϵ_{cc}) and ultimate (f_{ccu},ϵ_{ccu}) stress and strain values can be evaluated analytically.

For a column retrofitted by steel angles and battens, the confinement action exerted by the steel jacketing sums up with that of stirrups (Fig. 3a), producing different confinement levels over the cross-section. However, given that the steel jacketing confining action is prevailing, the model provides the use of a single concrete stress–strain law for the entire section. This assumption has demonstrated to be sufficiently reliable in comparison with experimental results [1–3].

The lateral confinement pressures $f_{le,x}$ and $f_{le,y}$ along the two direction of the cross-section (Fig. 3b) are evaluated as:

$$f_{le,x} = k_e \cdot \rho_{st,x} \cdot f_y ; f_{le,y} = k_e \cdot \rho_{st,y} \cdot f_y \quad (1)$$

in which the calculation of the transverse reinforcement volumetric ratios $\rho_{st,x}$ and $\rho_{st,y}$ consider both the contribution of internal and external transverse reinforcement as:

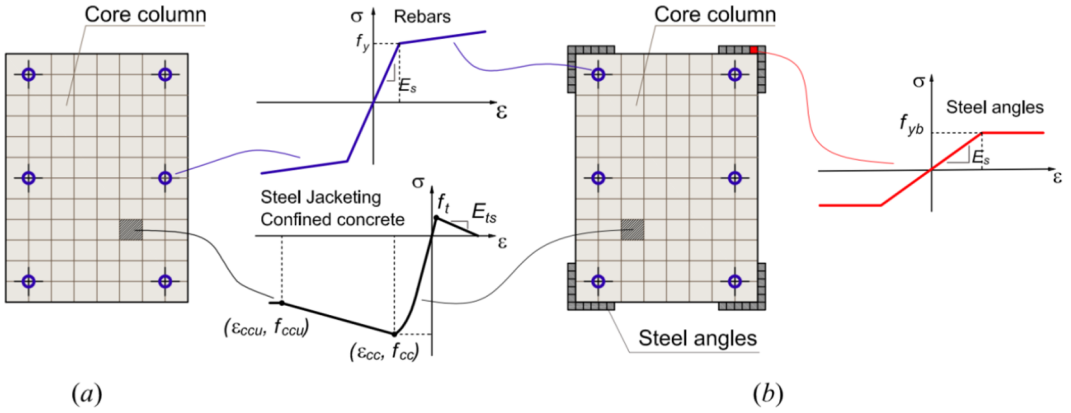

Fig. 2. Modelling of steel-jacketing in fiber-section elements: (a) steel-jacketing confinement action only; (b) steel-jacketing confinement and flexural resistance.

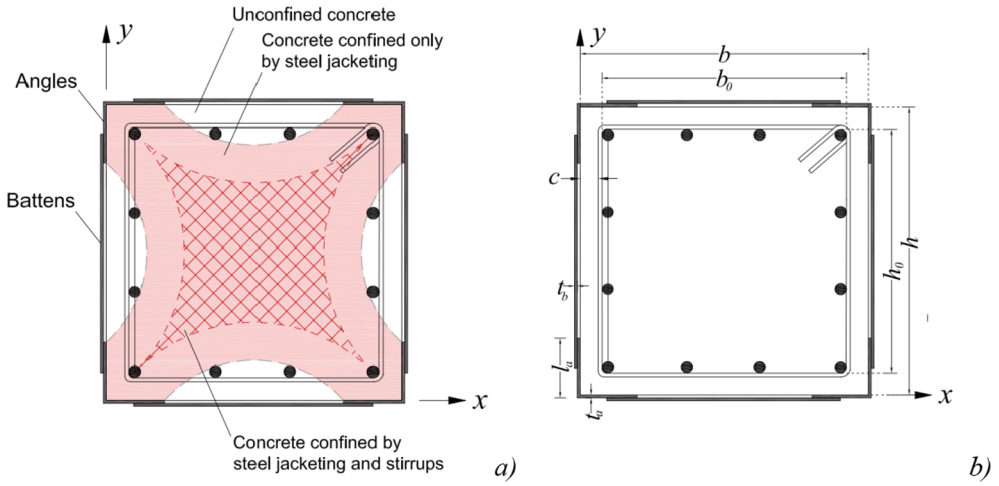

Fig. 3. Configuration of the cross-section of a column reinforced by steel jacketing: (a) effectively confined area by stirrups and steel jacketing; (b) geometric arrangement.

$$\rho_{st,x} = \frac{n_{bx} A_{st,x} b_0}{s b_0 h_0} + \frac{2A_{sb,e} b}{s_b b h}; \quad \rho_{st,y} = \frac{n_{by} A_{st,y} h_0}{s b_0 h_0} + \frac{2A_{sb,e} h}{s_b b h} \tag{2}$$

In Eq. (1) the coefficient k_e expresses the effectively confined area through the expression:

$$k_e = \left(1 - \frac{s_b - \phi_{st}}{2b_0}\right)\left(1 - \frac{s_b - \phi_{st}}{2h_0}\right) \tag{3}$$

In Eqs. (2) and (3) b is the cross-section base and h its height, $b_0 = b\text{-}2c$ and $h_0 = h\text{-}2c$, being c the width of the concrete cover, n_{bx} and n_{by} are the number of stirrups arms along x and y and $A_{st,x}$ and $A_{st,x}$ the respective areas, ϕ_{st} is the diameter of stirrups, s and s_b are the spacing of the internal hoops and external battens respectively. The term $A_{sb,e}$ represents the mechanically equivalent transverse area of battens and is calculated as:

$$A_{sb,e} = A_{sb}\frac{f_{yb}}{f_y} \tag{4}$$

where A_{sb} is the actual transverse area of a batten. In order to provide an automated determination of confinement parameters, confined peak stress (f_{cc}) and strain (ε_{cc}) and the ultimate stress (f_{ccu}) and strain (ε_{ccu}) are here evaluated by using the expressions provided by Razvi and Saatcioglu (1992) [26] instead of Mander et al. (1988) [27] model. In detail:

$$f_{cc} = f_c + k_1 f_{le} \tag{5}$$

where with reference to Fig. 3b, f_{le} and k_1 are obtained as:

$$f_{le} = \frac{f_{le,x} b_0 + f_{le,y} h_0}{b_0 + h_0}; \; k_1 = 6.7 f_{le}^{-0.17} \tag{6}$$

The confined peak strain ε_{cc} and the confinement factor K are finally evaluated as:

$$\varepsilon_{cc} = \varepsilon_c(1 + 5K); \quad K = k_1\frac{f_{le}}{f_c} \tag{7}$$

The linear softening branch is obtained by joining the peak stress–strain point (f_{cc}, ε_{cc}) with the point at which the compressive strain is reduced by 15% (f_{cc85}, ε_{cc85}). This point is individuated by:

$$f_{cc85} = 0.85 f_{cc}; \quad \varepsilon_{cc85} = 0.0036 + 260\rho_{st}\varepsilon_{cc} \tag{8}$$

where in order to include the effect of the steel jacketing, the term ρ_{st} is modified as follows:

$$\rho_{st} = \frac{A_{st,x} + A_{st,y} + 4A_{sb,e}}{\tilde{s}\,(b_0 + h_0)} \tag{9}$$

while $\tilde{s}$ represents the average stirrups/battens spacing that is proposed to calculate as:

$$\tilde{s} = \frac{s + s_b}{2} \tag{10}$$

The stress–strain curve becomes constant after the achievement of an 80% reduction of f_{cc}. Considering the linearity of the softening branch, the ultimate stress–strain parameters (f_{ccu}, ε_{ccu}) can be obtained as:

$$f_{ccu} = \alpha f_{cc} \tag{11}$$

$$\varepsilon_{ccu} = \varepsilon_{cc} + \frac{(1-\alpha)(\varepsilon_{cc85} - \varepsilon_{cc})}{0.15} \tag{12}$$

where $\alpha = 0.2$. For the current case it assumed that the conventional crushing of concrete fibers occurs when f_{cc} is reduced by 30%. Therefore parameters $f_{cc,cr}$ and $\varepsilon_{cc,cr}$ can be evaluated by Eqs. (11) and (12) by setting $\alpha = 0.7$.

Samples of the resulting stress–strain response in compression for a reference column cross-section fibers are reported in Fig. 4 considering the non-retrofitted case and the cases of steel-jacketing reinforcement with different battens spacing. Geometric and mechanical details of the reference cross-section and steel-jacketing details are reported in Table 1.

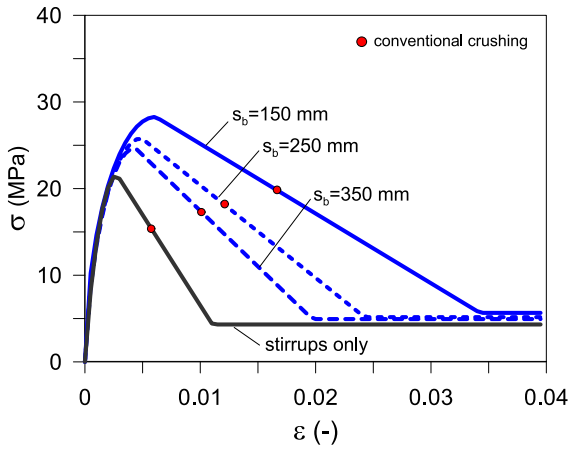

Fig. 4. Sample of stress–strain response of concrete in compression for a reference column (Table 1) with and without steel jacketing.

Table 1
Geometric and mechanical detail of the samples illustrated in Fig. 4.

Reinforced concrete column properties				
b (mm)	h (mm)	c (mm)	s (mm)	f_y (mm)
500	500	30	200	455
Steel jacketing properties				
$l_b \times t_b$ (mm × mm)	l_a (mm)	t_a (mm)	s_b (mm)	f_{yb} (mm)
50 × 5	10	5	150/250/350	275

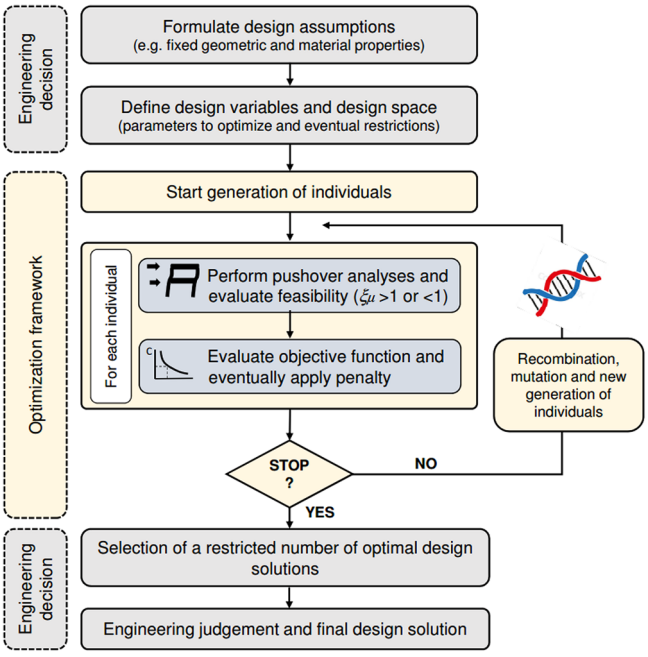

Fig. 5. Flowchart of the optimization process.

3. Design optimization framework

3.1. Operating principles of the optimization framework

The proposed optimization framework works by connecting the Matlab® genetic algorithm (GA) tool with a FE structural model developed with the OpenSees software platform. The framework is aimed at minimizing an objective function built by computing the retrofitting costs as a function of the defined design variables (number and location of retrofitted columns and respective battens spacing) associated with the steel jacketing reinforcement. A flowchart of the optimization procedure is shown in Fig. 5. The procedure starts with the engineering design choices about fixed geometric and material properties. Then, the individuated design variables are eventually limited to a restricted design space (e.g. limit the number of columns involved in the optimization process). The phase of restriction of the design space, fundamental to reduce the number of possible combinations of design variables and reduce computational effort, has to be carried out specifically for each case. After this point, the optimization algorithm starts generating the first population of random individuals. Each individual is representative of one model of the structure having one possible combination of the design variables. The feasibility of each solution is assessed by carrying out one (o more) pushover analyses and computing the ratios between ductility capacity and demand (μ_c/μ_d) in the framework of the N2 method. This allows reasonable computational effort and concise identification of seismic performance with a unique parameter. The retrofitting cost of each solution is then computed by evaluating the objective function. The cost is eventually incremented by a penalty factor, fictitiously increasing the amount if one or more solutions are unfeasible ($\mu_c/\mu_d < 1$). For each generation the GA will combine the best individuals through the crossover and mutation operators. The optimization framework is stopped when the optimization algorithm does not provide significant improvements in terms of cost minimization. A final engineering judgment phase is necessary to assess potentially equivalent optimal solutions in terms of practice engineering feasibility and to eventually make final design corrections.

The definition of the population size is fundamental to the effectiveness of the optimization, especially in terms of computational effort (each individual requires performing a pushover analysis), but this extremely varies case by case. Therefore, the common rule of assuming the population as 10 times the number of variables may result significantly time-consuming to this application. A more reasonable compromise can be found assuming the population size in the range 2-5 times the size of the design vector.

The recombination phase is performed using a scattered crossover operator which generates a random binary vector, having size as the design vector, used to select the genes from the parents. The gene is taken from the first parent where the vector is a 1, and from the second parent where the vector is a 0. A Gaussian mutation operator is finally applied to the child vectors.

3.2. General assumptions of the optimization framework and definition of the design variables

In order to restrict the design optimization variables as much as possible, the following basic assumption are made for the steel jacketing retrofitting system:

(i) The angles are constituted by L-shaped steel profiles having fixed lateral length (l_a) and thickness (t_a) for all the retrofitted columns
(ii) The battens are constituted by rectangular plates having fixed thickness (t_b) and width (w_b) for all the retrofitted columns.
(iii) Battens spacing is the same for all the retrofitted columns.

In consideration of Eqs. (1)–(12), the consequence of the aforementioned assumptions is that the battens spacing (s_b) remains the only variable defining the effect of the jacketing on confinement.

Therefore the design vector ($\boldsymbol{b}$) is formulated as:

$$\mathbf{b} = \begin{pmatrix} s_b \\ \mathbf{p} \end{pmatrix} \tag{13}$$

where s_b is a scalar belonging to the interval S so defined:

$$s_b \in S = [s_{b,\min} \quad s_{b,\max}] \tag{14}$$

in which $s_{b,\min}$ and $s_{b,\max}$ are the minimum and maximum allowed battens spacings, while $\boldsymbol{p}$ is a vector collecting the positions of the columns included in the design space having the following form:

$$\mathbf{p} = (\ \ldots \quad \ldots \quad c_{ij} \quad \ldots \quad \ldots\ )^T \tag{15}$$

The elements belonging to $\boldsymbol{p}$ have the generic shape c_{ij} elements, where i represents the position of the column with reference numbering in plan, and j represents the storey. The c_{ij} elements are binary elements assuming the value 0 if the column is not retrofitted and 1 if the column is retrofitted. Therefore, c_{ij} elements belong to the binary set named C and so defined:

$$c_{ij} \in C = (0 \ \ 1) \tag{16}$$

During the optimization process, the GA generates the population of

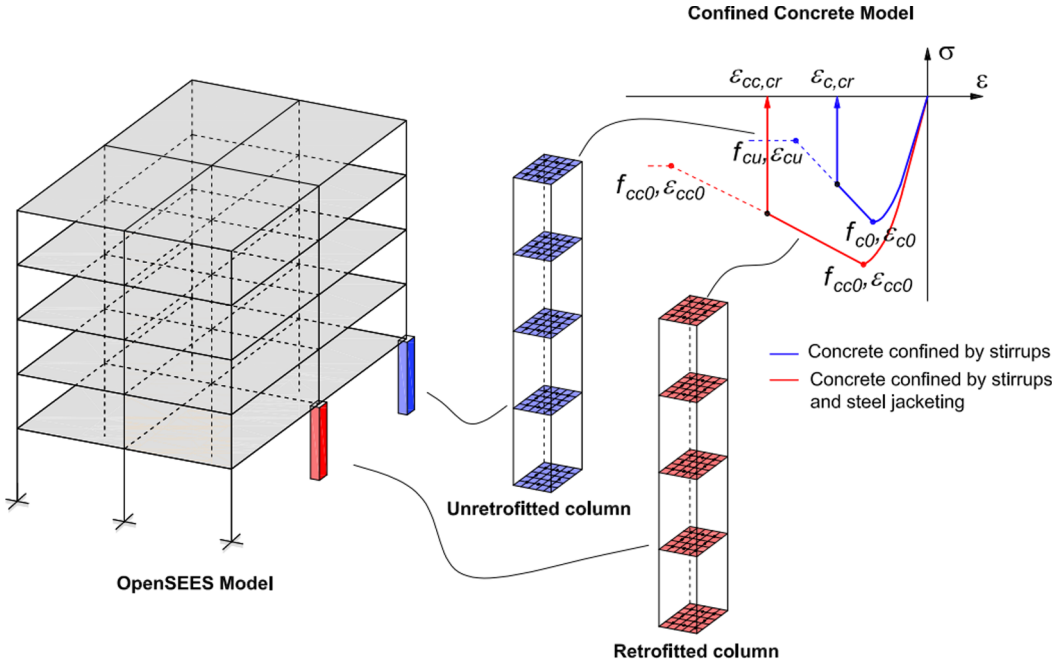

Fig. 6. Definition of the fiber-section elements in OpenSees with and without considering steel-jacketing reinforcement.

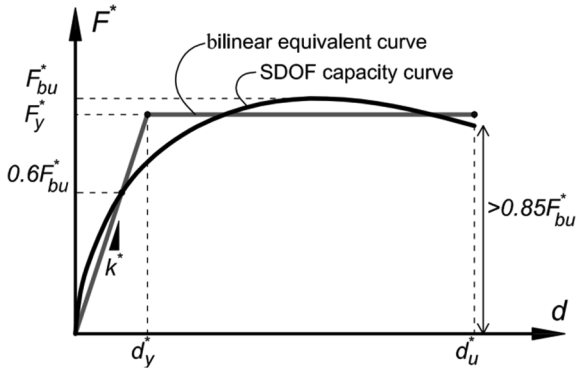

Fig. 7. Equivalent SDOF capacity curve and bilinear equivalent curve.

individual by assigning the elements of the ***b*** vector, and each ***b*** vector will characterize an individual (namely a model) with specific position and stirrups spacing of the retrofitted columns.

3.3. General model implementation options within the optimization framework

Reinforced concrete frame elements (beams and columns) are modelled adopting distributed plasticity force-based elements with five Gauss-Lobatto integration points available in OpenSees (Fig. 6). A "Concrete02" uniaxial material model is attributed to the cross-section fibers. For sake of simplicity it is assumed that the effect of confinement is extended to the whole cross-section (Fig. 6) both for the cases of columns with and without steel jacketing reinforcement. This simplified assumption is used to obtain a formal consistency with the confinement model in the case of concrete confined by stirrups and steel jacketing (Campione et al. 2017 [1]) which provides uniform confinement over the cross-section. In order to simulate the crushing of the cross-section fibers, Concrete02 material is combined with "MinMax" material, which removes the contribution of a fiber when a specified strain threshold is achieved. For the current case, it is assumed that the crushing of fibers occurs in correspondence of the compressive strain (ε_{cr}) attained at a 30% reduction of the peak strength.

Therefore, parameters of concrete confined only by stirrups (f_{c0}, f_{cu}, ε_{c0}, ε_{cu}) and by stirrups and steel-jacketing (f_{cc0}, f_{ccu}, ε_{cc0}, ε_{ccu}) are first defined. After, the respective crushing strains $\varepsilon_{c,cr}$ and $\varepsilon_{cc,cr}$ are evaluated and imposed as strain limits in compression (Fig. 6). Confined concrete parameters for the RC elements confined only by stirrups are evaluated using the stress–strain model by Razvi and Saatcioglu (1992) [26]. As for the columns with steel jacketing retrofitting, confined concrete parameters are obtained following the approach by Montuori and Piluso (2009) [3] as described in the previous section.

Steel rebars are modelled using the "Steel02" (Giuffrè-Menegotto-Pinto) material model (elasto-plastic with linear strain hardening). Finally, floors are supposed to have rigid diaphragm behaviour by imposing diaphragm constraint at the nodes.

3.4. Processing of pushover results

Pushover curves obtained for each individual are processed in the framework of the N2 method [24], which is also provided by Eurocode 8 [28]. In order to determine the capacity/demand ductility ratios (μ_c/μ_d). The ductility demand (μ_d) of an inelastic single degree of freedom system (SDOF) can be obtained from the well-known relationships:

$$\begin{aligned} \mu_d &= (q^* - 1)\frac{T_C}{T^*} + 1 \quad \text{if } T^* \leqslant T_C \\ \mu_d &= q^* \qquad\qquad\qquad\quad \text{if } T^* > T_C \end{aligned} \tag{17}$$

where T^* is the period of the equivalent SDOF system having mass m^*, and stiffness k^* and reduction factor q^* evaluated as:

$$T^* = 2\pi\sqrt{\frac{m^*}{k^*}}; \quad k^* = \frac{F^*_y}{d^*_y}; \quad q^* = \frac{S_{ae}(T^*)m^*}{F^*_y} \tag{18}$$

through the bilinearization of the SDOF capacity curve (Fig. 7), provided that $S_{ae}(T^*)$ is the elastic spectral acceleration of the same system.

The ductility capacity (μ_c) is still evaluated from the bilinear curve as:

$$\mu_c = \frac{d_u^*}{d_y^*} \tag{19}$$

The capacity/demand ratio (ξ_μ) is finally:

$$\xi_\mu = \frac{\mu_c}{\mu_d} \tag{20}$$

The coefficient ξ_μ is the final output of the processing of pushover curves and is used as a discriminating factor in the optimization process in order to establish if a single individual passes the verification check ($\xi_\mu \geq 1$) or not ($\xi_\mu < 1$). Different reference ξ_μ values can be eventually adopted if higher of lower target safety level are selected.

Pushover analysis is in general carried out at least for two orthogonal directions and two lateral load profiles (modal and uniform), and especially for irregular buildings, the number of analyses (n_a) is increased. In order to account for the results of more pushover analyses for a single individual, the ductility capacity/demand ratios obtained from each analysis ($\xi_{\mu i} = \mu_{c,i}/\mu_{d,i}$) can be combined to obtain the so defined overall capacity/demand index ($\tilde{\xi}_\mu$):

$$\tilde{\xi}_\mu = \begin{cases} \bar{\xi}_\mu & if\ \xi_{\mu,i} \geq 1 \quad \forall\ i \\ \dfrac{\bar{\xi}_\mu}{\bar{\xi}_\mu + \left(\frac{n_{a,u}}{n_a}\right)} & if\ \exists\ \ \xi_{\mu,i} < 1 \end{cases} \tag{21}$$

where $\bar{\xi}_\mu$ is the average capacity demand ratio evaluated as:

$$\bar{\xi}_\mu = \frac{1}{n_a}\sum_{i=1}^{n_a} \xi_{\mu,i} \tag{22}$$

while the term ($n_{a,u}/n_a$) is the ratio between the number ($n_{a,u}$) of analyses presenting unfeasible outcomes ($\xi_\mu < 1$) and the total number of pushover analyses (n_a). In this way, the evaluation of $\tilde{\xi}_\mu$ allows to connect the results of n_a pushover analyses to a single discriminant value, having as significance that if $\tilde{\xi}_\mu \geq 1$, all the performed analyses are feasible and $\tilde{\xi}_\mu$ simply represents the average of resulting capacity/demand ratio. On the contrary, if $\tilde{\xi}_\mu < 1$, at least one of the analyses is unfeasible. In this case the evaluation of $\tilde{\xi}_\mu$ is carried out considering major penalty as the number of unfeasible solutions increases with respect to the total number of analyses by means of the term $n_{a,u}/n_a$.

3.5. Definition of the objective function

The objective function monitors the retrofitting costs intended as the material costs and the manpower costs to realize column steel jacketing (C_{SJ}) and necessary works for demolition and reconstruction of plasters and masonry (C_M). The general form of the objective is therefore:

$$C = C_M + C_{SJ} \tag{23}$$

The cost C_M has been estimated considering a fixed amount (c_m) of 2000 € per reinforced column, hence:

$$C_M = n_c c_m \tag{24}$$

where n_c is the number of retrofitted columns. As regards C_{SJ}, this can be computed as:

$$C_{SJ} = c_s \sum_{i=1}^{n_c} W_{s,i} \tag{25}$$

where $W_{s,i}$ is the total weight of steel used to arrange a steel jacketing cage and c_s is the manpower and material cost per unit weight (estimated in 4.5 €/kg). For the current case, since all the columns have the same dimension, all the steel cages will have the same weight, therefore Eq. (25) becomes more simply:

$$C_{SJ} = n_c W_s c_s \tag{26}$$

where W_s is the fixed weight of the steel cage calculated as:

$$W_s = (V_A + V_B)\gamma_s \tag{27}$$

in which γ_s is the specific weight of steel (78.5 kN/m^3), and V_A is the total volume of steel angles applied at the corners of the columns, that is:

$$V_A = 8 \cdot l_a \cdot t_a \cdot l_c \tag{28}$$

l_c being the length of the column. Finally, V_B is the total volume of battens, which depends on their spacing as follows:

$$V_B = 2(V_{bx} + V_{by})\left(\frac{l_c}{s_b}\right) \tag{29}$$

and where V_{bx} and V_{by} are the volumes of singles batten along the two orthogonal directions, that is:

$$V_{bx} = t_b l_b (b - l_a); \quad V_{by} = t_b l_b (h - l_a) \tag{30}$$

For the case of square columns, where $V_{bx} = V_{by} = V_b$, Eq. (29) becomes:

$$V_B = 4V_b\left(\frac{l_c}{s_b}\right) \tag{31}$$

3.6. Definition of the penalty function

The search strategy adopted by the GA considers the fitness of a solution and is unaffected by any violation of problem constraints. For the current case, the feasibility of a solution is represented by the capacity/demand ratio (ξ_μ or $\tilde{\xi}_\mu$), which is determined as shown in the previous section. In order to take into account feasibility of a solution, and therefore the possible violation of a constraint, a penalty function is introduced. This can be expressed by changing the objective function (C) into the function F as follows:

$$F = C + \Pi \tag{32}$$

where Π is the penalty function having the following form:

$$\Pi = \begin{cases} 0 & if\ \ \tilde{\xi}_\mu \geq 1 \\ C_{\max}\left(\frac{1}{\tilde{\xi}_\mu}\right)^3 & if\ \ \tilde{\xi}_\mu < 1 \end{cases} \tag{33}$$

and in which C_{max} is the maximum possible retrofitting cost (reinforcement of all first and second floor columns with $s_b = 150$ mm). This means that if a solution is feasible, no penalty is assigned ($F = C$). On the contrary, if a solution is not feasible, the current cost is fictitiously increased by C_{max} multiplied by the factor $(1/\tilde{\xi}_\mu)^3$, which takes into account the distance of the current solution from the feasibility ($\tilde{\xi}_\mu = 1$). A graphical exemplification of the penalty function is illustrated in Fig. 8 as a function of the term $1/\tilde{\xi}_\mu$.

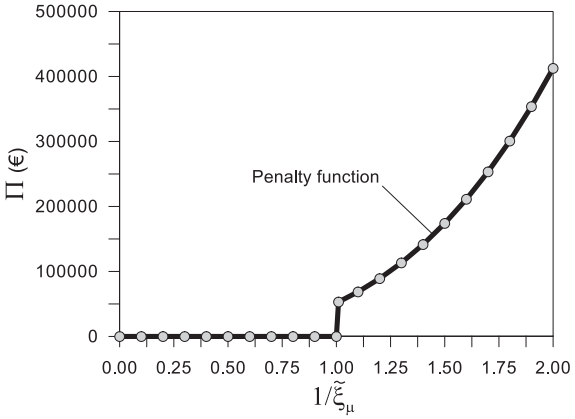

Fig. 8. Penalty function.

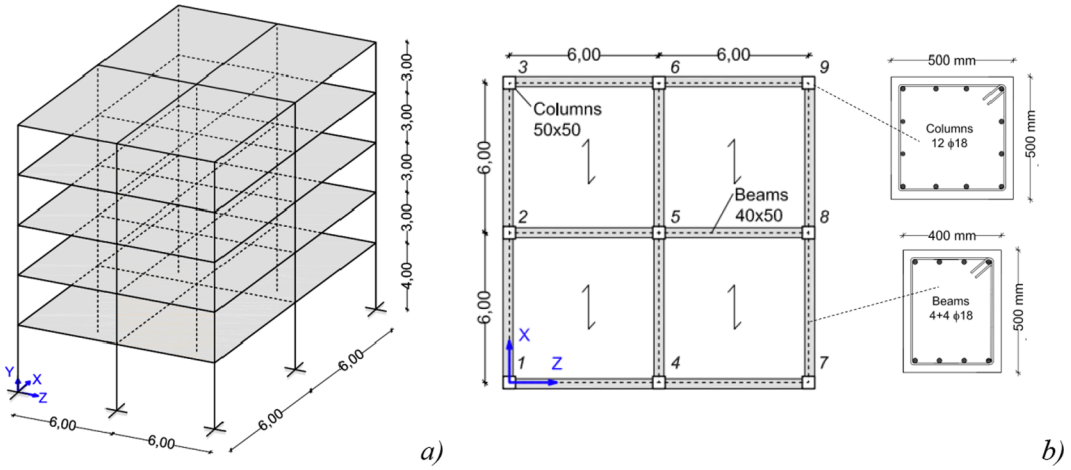

Fig. 9. Geometrical dimensions of the case study structure: (a) 3D frame view; (b) dimensions in plan.

Table 2
Reinforcement details of beams and columns.

RC members	$b \times h$ (mm)	Longitudinal reinforcement	Transverse reinforcement
Beams	400 × 500	4 + 4 ϕ18	ϕ6/200 mm
Columns	500 × 500	12 ϕ18	ϕ6/200 mm

4. Case study structure and specific design optimization assumptions

The case study building consists of a five-storey two-bays reinforced concrete structure designed to resist only gravity loads. The structure (Fig. 9a) has polar symmetry in plan and is regular in elevation. Dimensions in plan are represented in Fig. 9b as well as dimensions of beams and columns. The structure is supposed to be arranged with poor resistance concrete having average unconfined strength $f_{c0m} = 20$ MPa. Steel rebars have average yielding strength $f_y = 455$ MPa and strain hardening ratio is supposed being $\eta = 0.01$ [29]. Reinforcement details of beams and columns are listed in Table 2. The building is supposed being located in Cosenza (Italy), soil type C. The reference nominal life (V_N) is of 100 years. The resulting return period is $T_R = 975$ years.

It supposed that jackets are applied without realizing moment-resisting end connections and that fictional contribution to flexural resistance is neglected. Therefore, angles are not included in the cross-section assembly.

Vertical loads are assigned by point loads at the top of each column as function of the respective tributary areas in plan. The total weight of each floor is 1440 kN.

Since the study is mainly focusing on testing the optimization framework, beam-column joint nonlinear behaviour is not explicitly modelled. This does not limit the eventual adoption of specific models (e.g. Lowes et al. (2003) [30]). Moreover, in order to reduce computational effort, pushover analyses are carried out by considering only a uniform profile for lateral loads. Optimization results can be finally checked with any profile and direction.

The general assumptions *i-iii* presented in Section 3.2 are applied as follows:

(i) Steel angles have lateral length $l_a = 100$ mm and thickness $t_a = 5$ mm.
(ii) The thickness of the battens (t_b) is 5 mm, the width (w_b) is 50 mm.
(iii) Yielding strength of steel angles and battens is $f_{yb} = 275$ MPa and their spacing is the same for all the retrofitted columns.

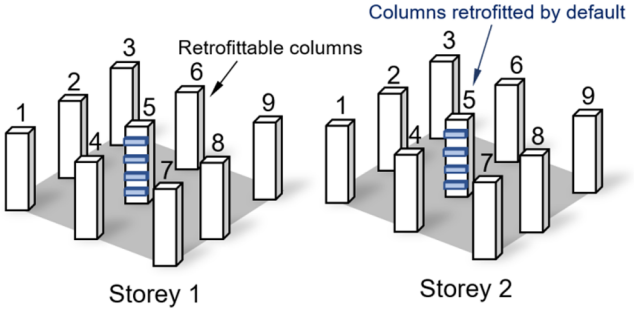

Fig. 10. Scheme of the design space.

Moreover, as suggested in the by the general formulation of the optimization framework, the following restrictions are applied to reduce the dimension of the designs space:

(iv) Retrofitted columns can be only located within the first the second floor.
(v) Internal columns (position 5 in Fig. 10) at the first and second floors are always retrofitted.
(vi) Minimum and maximum spacings between the battens are 150 and 400 mm respectively.

Assumption *iv* is justified by the fact that the maximum deformation demand is expected at the first two (of five) stories. Assumption *v* arises from the observation that the internal columns are supporting the majority of gravity loads and therefore suffer the major reduction of the deformation capacity. Assumption *vi* is done to limit possible battens spacing into a feasible range of values.

Based on the aforementioned assumptions, the design vector ($\boldsymbol{b}$) components (s_b and $\boldsymbol{p}$) are specialized as:

$$s_b \in S = [150 \quad 400] \tag{34}$$

and $\boldsymbol{p}$ is a 16×1 vector collecting the positions of the columns at the first two floors, excluding the central ones, and having the following shape:

$$\mathbf{p} = (c_{11} \;\; c_{21} \;\; c_{31} \;\; c_{41} \;\; c_{61} \;\; c_{71} \;\; c_{81} \;\; c_{91} \;\; c_{12} \;\; c_{22} \;\; c_{32} \;\; c_{42} \;\; c_{62} \;\; c_{72} \;\; c_{82} \;\; c_{92})^T \tag{35}$$

The resulting size of the design space is then of 17 variables. A

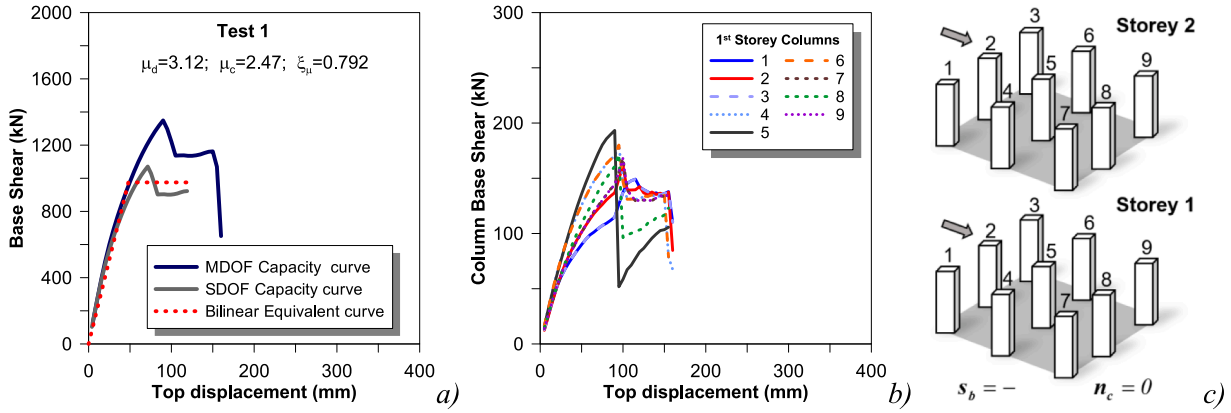

Fig. 11. Preliminary Test 1: (a) Overall pushover capacity curves; (b) First storey columns capacity curves; (c) Structural configuration at the first two stories.

schematic representation of the design space is illustrated in Fig. 10. In consideration of the general recommendations given in section 3.1, the population size is reasonably fixed as 3 times the size of the design vector (50 individuals per generation).

5. Results of the optimization

5.1. Preliminary tests

Before starting with the optimization process of the retrofitting, the seismic performance of the reference structure has been tested without any retrofit and under different trial retrofitting configuration. This is first done to get a reference point about the safety of the structure as built. Secondly, the test of a number of trial retrofit configurations allows comparing cost/performance results with those of the solution found through the optimization framework solution. Given the polar symmetry of the structural configuration, a single (one direction) pushover analysis is carried out for each configuration in order to reduce the computational effort to obtain the capacity/demand ratio $\tilde{\xi}_{\mu}$, which becomes coincident to ξ_{μ}.

The five preliminary tests provide the following configurations:

- Test 1: No retrofitting (as built);
- Test 2: Retrofitting of all 1st and 2nd floor column with $s_b = 150$ mm;
- Test 3: Retrofitting of all 1st floor columns and 2nd floor central column with $s_b = 150$ mm;
- Test 4: Retrofitting of all 1st floor and 2nd floor central columns with $s_b = 250$ mm and
- Test 5: Retrofitting of all 1st floor and 2nd floor corner columns and 1st floor and 2nd floor central column with $s_b = 250$ mm.

Results of the tests are illustrated in Figs. 11–15 in terms of total base shear and column base shear against top displacement. Results in terms of ductility capacity/demand ratios and retrofitting costs are also reported in Tables 3 and 4.

Results of the tests allowed making important considerations about seismic performance of the structure with and without the steel jacketing retrofitting. It can be first observed that the as-built configuration (Test 1) has shown low displacement ductility capacity, presenting a ξ_{μ} ratio of 0.792. This was mainly related to the fact the structure suffered a significant resistance drop (Fig. 11) associated with the collapse of the central column (5) carrying out the largest portion of vertical loads. The overall retrofitting of the first and second floor (Test 2, Fig. 12) significantly improved the response ($\xi_{\mu} = 1.72$) but was associated with noticeable intervention costs (51578.33 €) to retrofit all the 18 columns. The retrofitting of all the columns at the first floor (Test 3, Fig. 13) was not sufficient to pass the verification check ($\xi_{\mu} = 0.931$) but was interesting to observe that, in comparison, tests 4 and 5 showed more effective performances by retrofitting the same number of columns ($n_c = 10$) at specific position of the first and the second floor even with a larger battens spacing. In the last chase, in fact, the structure was retrofitted with an intervention cost of 27,170.98 € obtaining a capacity/demand ratio of $\xi_{\mu} = 1.03$. A further meaning coming from the

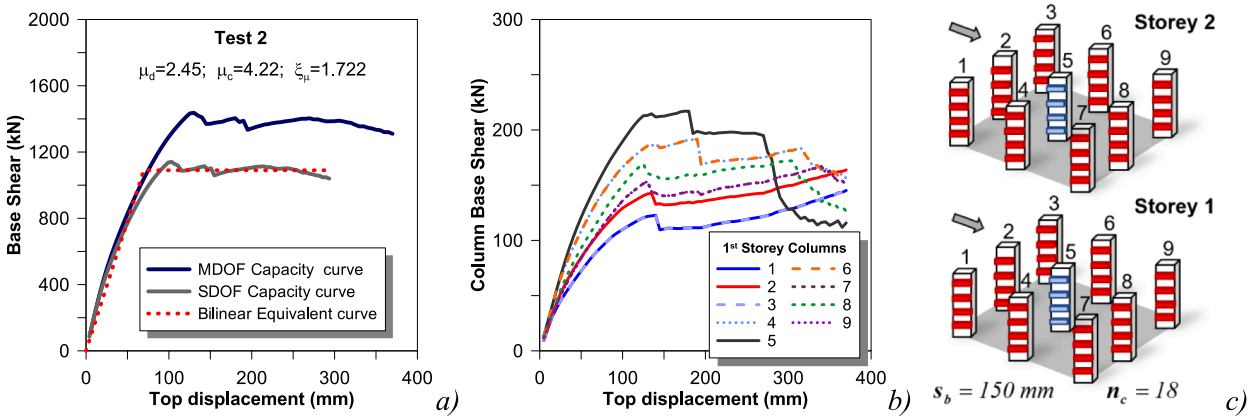

Fig. 12. Preliminary Test 2: (a) Overall pushover capacity curves; (b) First storey columns capacity curves; (c) Structural configuration at the first two stories.

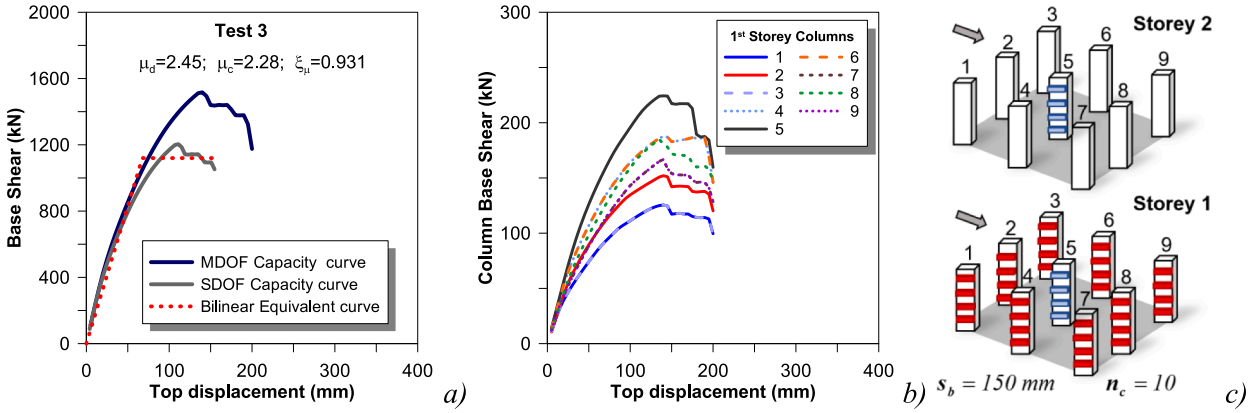

Fig. 13. Preliminary Test 3: (a) Overall pushover capacity curves; (b) First storey columns capacity curves; c) Structural configuration at the first two stories.

preliminary test is that a reduction of the number of the retrofitted columns or of the battens spacing is not necessarily associated with a reduction of safety. On the contrary, increases in safety levels can be combined with cost-saving by an adequate positioning of the reinforcement, giving the idea that engineering optimization of such problems becomes fundamental, in the case of large structures.

5.2. Optimization results

Given the polar symmetry of the structural configuration, the optimization framework is applied considering only one direction of action of the lateral force profile. This allows, on the one hand, a reduction of the computational effort necessary to obtain the optimal solution, which can be simply generalized to other directions based on simple symmetry considerations. On the other hand, this simplified decoupling of the optimization problem misses to check is if the final solution supposed for all directions represents also the optimal solution that would have been found by the application of the standard optimization framework. However, both in the case of simplified or full optimization, results of such framework must be intended as a suggestion to the designer who will find a practical final compromise.

Under these assumptions, the optimization process for the reference structure has shown the convergence history illustrated in Fig. 16, where the single fitness evaluations are reported against the fitness value (retrofitting cost) obtained from Eq. (34). In the same diagram, the moving average trend is also reported. It can be observed that the algorithm tends to a stable solution after about 870 evaluations of individuals. As a counterpart of the retrofitting cost trend, the diagram in Fig. 17 shows the history of the capacity/demand ratio (ξ_μ) values over the evaluations. It can be noted that the GA starts finding only feasible solutions (on average) after 600 iterations and also that ξ_μ approaches to values close to 1 by going ahead with the iterations, indicating that optimized solutions are also associated with major exploitation of the retrofitting intervention.

The objective function values assumed by the single individuals are also illustrated in Fig. 18a as a function of ξ_μ. The same values are reported in Fig. 18b using a logarithmic scale in order to allow graphical individuation of the optimal solution. In Fig. 18a and b, the vertical line passing through $\xi_\mu = 1$ individuates the sets of feasible and unfeasible solutions. Another vertical line passing through the point individuating the optimal solution (Fig. 18b), divides feasible solutions into two sub-sets. This distinction allows individuating a number of solutions presenting higher retrofitting costs associated with lower safety levels, demonstrating that cost minimization is not directly correlated with a reduction of safety levels. At the same time this means that the optimization process allows discarding a number of ineffective retrofitting solutions for which larger costs are associated with lower safety.

The optimal solution of the one direction optimization is found at iteration 821. The latter provides retrofitting of central columns 2 and 8 (Fig. 19) at the first floor (besides the central internal column at the first and the second floor) with a batten spacing $s_b = 250$ mm and $\xi_\mu = 1.014$ (details are reported in Table 5). From an engineering point of view, the solution found by the optimization framework is

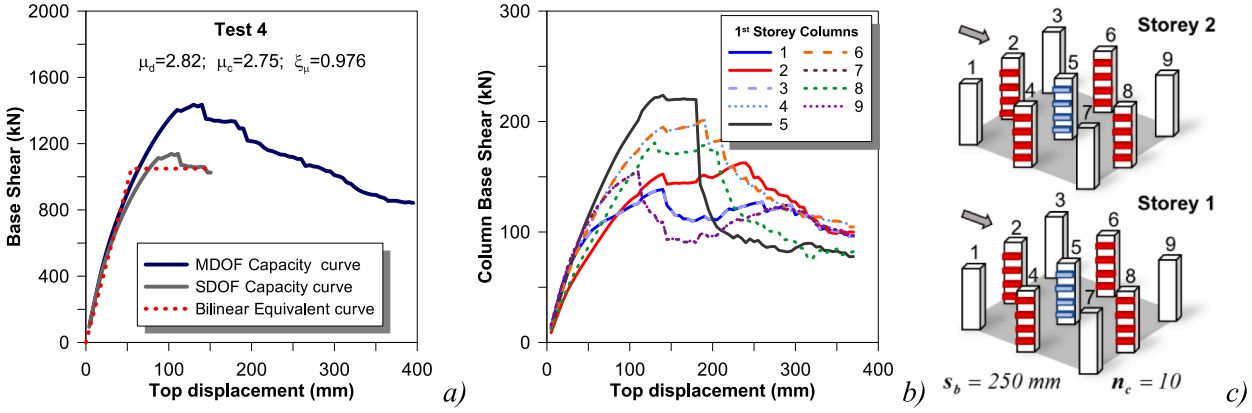

Fig. 14. Preliminary Test 4: (a) Overall pushover capacity curves; (b) First storey columns capacity curves; c) Structural configuration at the first two stories.

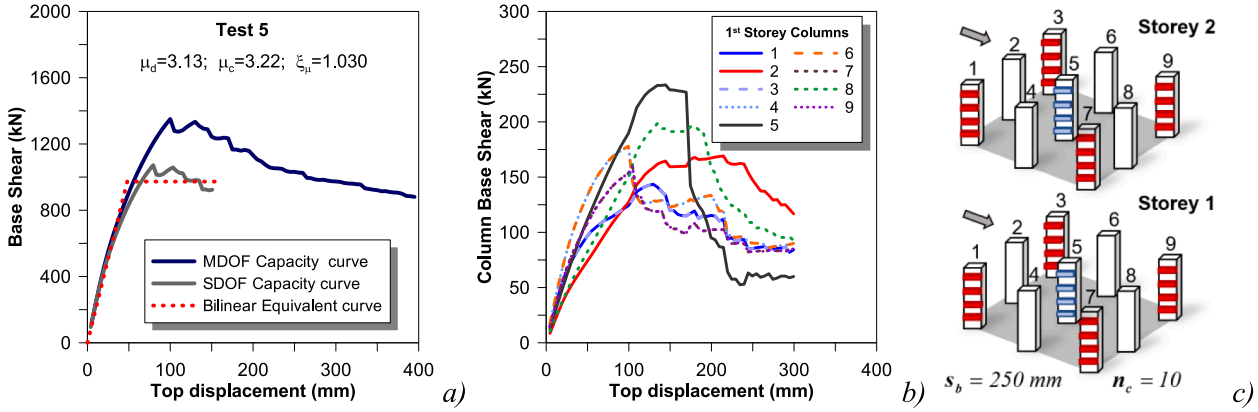

Fig. 15. Preliminary Test 5: (a) Overall pushover capacity curves; (b) First storey columns capacity curves; (c) Structural configuration at the first two stories.

Table 3
Results of preliminary tests.

Test	μ_d (–)	μ_c (–)	ξ_μ (–)	s_b (mm)	n_c	C (€)	Verif. check
1	3.120	2.470	0.792	–	0	–	No
2	2.450	4.220	1.722	150	18	51578.33	Yes
3	2.451	2.280	0.931	150	10	28654.63	No
4	2.815	2.748	0.976	250	10	27170.98	No
5	3.125	3.220	1.030	250	10	27170.98	Yes

Table 4
Results of the optimization.

Direction	μ_d (–)	μ_c (–)	ξ_μ (–)	s_b (mm)	n_c	C (€)	Verif. check
Z+	3.041	3.085	1.014	250	4	10868.39	Yes
All directions	2.805	2.835	1.010	250	6	16302.59	Yes

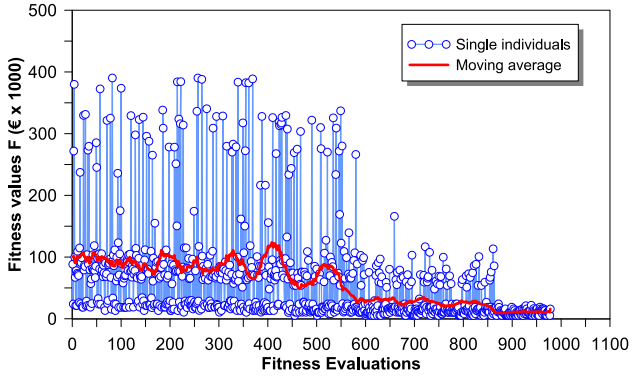

Fig. 16. Convergence history of the cost over the fitness evaluations.

reasonable, in fact, columns 2 and 8, carry more gravity load with respect to corner columns, and therefore suffer major reduction of curvature ductility. Moreover, in comparison with columns 4 and 6, columns 2 and 8 undergo larger axial force variation to equilibrate the base moment introduced by lateral forces. This has as effect a reduction of flexural capacity of column 2, and on the other hand, a reduction of curvature ductility of column 8.

As mentioned in the previous section, the optimal solution found refers to a pushover force profile acting along Z positive (negative) direction. In this case, given the polar symmetry of the structure in plan

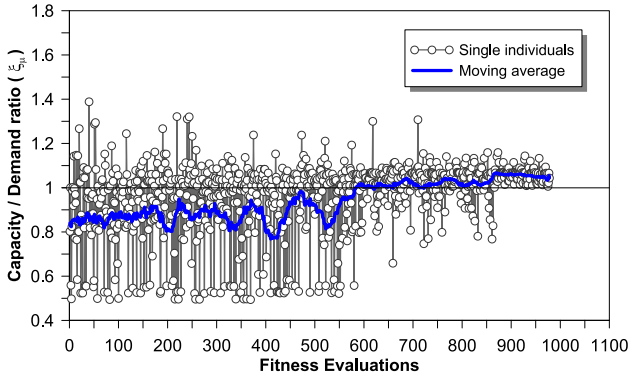

Fig. 17. History of the capacity/demand ratio (ξ_μ) values over the fitness evaluations.

and elevation, it can be simply is supposed to retrofit in the same way (s_b = 250 mm) column 6 and 4 in order to face seismic demand along X direction.

The so defined final retrofitting configuration performance is illustrated in Fig. 20 and Table 5. The capacity demand ratio finally obtained is ξ_μ = 1.01, while the overall cost of the intervention is 16302.59 €. It is noteworthy observing that the obtained cost is reduced by 40% with respect to the best solution found with preliminary tests (Test 5). However, in the face of this, the ξ_μ factor finally obtained (1.01) differs only by 2% with respect to that obtained in test 5 (1.03) with a retrofitting cost of 27170.98 €. The computational cost required for this case-study retrofitting optimization mainly depended on the time needed to perform the single pushover analyses. For the current case, this was about 0.5 min. The resulting computational time was then of about 8 h. Although this can be considered a non-negligible time consumption, the advantages in terms of economical cost savings certainly justify the application of this optimization framework especially. This is even more true for larger reinforced concrete frames structures, where retrofitting and downtime costs become a crucial issue.

6. Effectiveness of the optimization framework in case of structural irregularities

In order to test the effectiveness of the proposed framework even in the case of more complex structural configurations, the retrofitting optimization of the previously analysed case study structure has been carried out again by introducing irregularities in plan and elevation induced by masonry infills. In detail, solid masonry infills are supposed

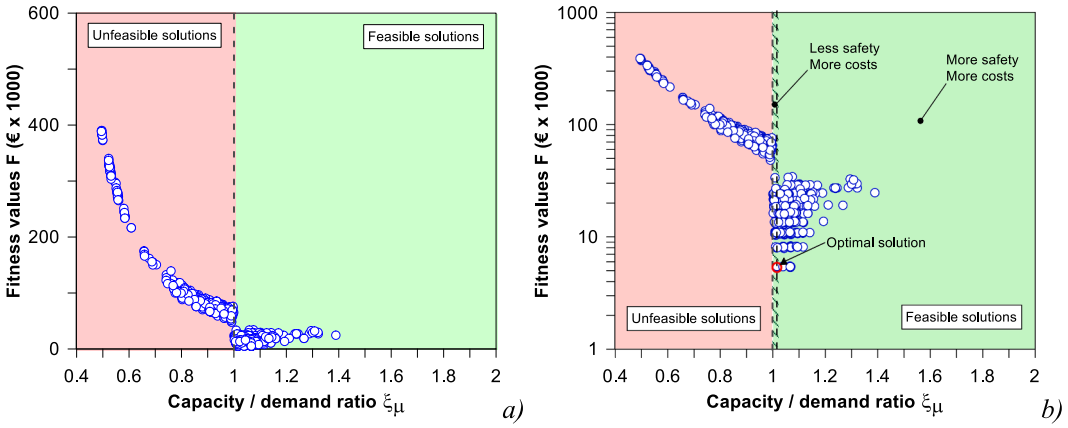

Fig. 18. Objective function values as a function of ξ_μ in: (a) linear scale; (b) logarithmic scale.

being placed only in one of the external frames at all storeys except for the first (Fig. 21a). Infills are modelled as fiber-section struts according to the model by Di Trapani et al. [31–34] (Fig. 21b). The model provides using a concrete-type compression-only stress–strain relationship defined by the equivalent parameters of peak strength (f_{md0}), ultimate strength (f_{mdu}), peak strain (ε_{md0}) and ultimate strain (ε_{mdu}). Geometric and mechanical parameters of the struts reported in Table 5 are consistent with a clay hollow masonry infill having thickness $t = 250$ mm, elastic modulus $E_m = 6400$ MPa, compressive strength $f_m = 8.66$ MPa and shear strength $f_{vm} = 1.07$ MPa.

In the so defined structural configuration, the lateral response of the system is significantly modified along Z direction, due to the increase in stiffness and the migration of the stiffness center toward the infilled frame. In addition, infills significantly reduce interstorey drift demand of the surrounding frames with respect to that of the first floor. On the contrary, the behaviour along X direction remains similar to that of the bare frame configuration. This is confirmed by the preliminary push-over analyses carried out for the non-retrofitted structure illustrated in Fig. 22, which also highlight a major vulnerability along Z direction ($\xi_\mu = 0.535$).

The individuation of the optimal retrofitting solution is in this case not obvious, but it is reasonable starting a tentative optimization along the direction of the infills (Z direction) which is also the weakest. Design assumptions about research space (Section 4) are maintained in this case. In addition, the columns at the sides of the infills at the second storey are removed from the design vector, because of the reduced drift demand. The $\boldsymbol{p}$ vector is therefore:

$$\mathbf{p} = (c_{11}\ \ c_{21}\ \ c_{31}\ \ c_{41}\ \ c_{61}\ \ c_{71}\ \ c_{81}\ \ c_{91}\ \ c_{22}\ \ c_{32}\ \ c_{62}\ \ c_{82}\ \ c_{92})^T \quad (36)$$

The resulting size of the design space is then of 14 variables. The population size is maintained 50 individuals per generation. The optimization process has shown the convergence history illustrated in Fig. 23a. It can be observed that the algorithm tends to a stable solution more rapidly (about 550 evaluations). This is due to the further restriction of the design space. The trend of capacity/demand ratio over the fitness evaluation is shown in Fig. 23b. Also in this case ξ_μ approaches to values close to 1, confirming the maximum exploitation of the retrofitting intervention.

The optimal solution found (Z direction) provides retrofitting of columns 6 and 9 at the first storey, in the frame opposite to that containing the infills and of column 4 at the first storey, in the frame including the infills at the upper stories (Fig. 24). The battens spacing is $s_b = 250$ mm.

The optimal solution found results consistent with the expected structural behaviour. In fact, the reinforcement of column 6 and 9 can be associated with the major torsional demand around the new stiffness center, which is closer to the infilled frame. On the other hand, the reinforcement of column 4 confirms a major displacement demand at the first storey due to the stiffening and strengthening action of the upper stories infills. The resulting capacity/demand ratio is $\xi_\mu = 1.015$.

The final retrofitting configuration is found by supposing that, due to symmetry, even column 3 is retrofitted to face lateral actions acting

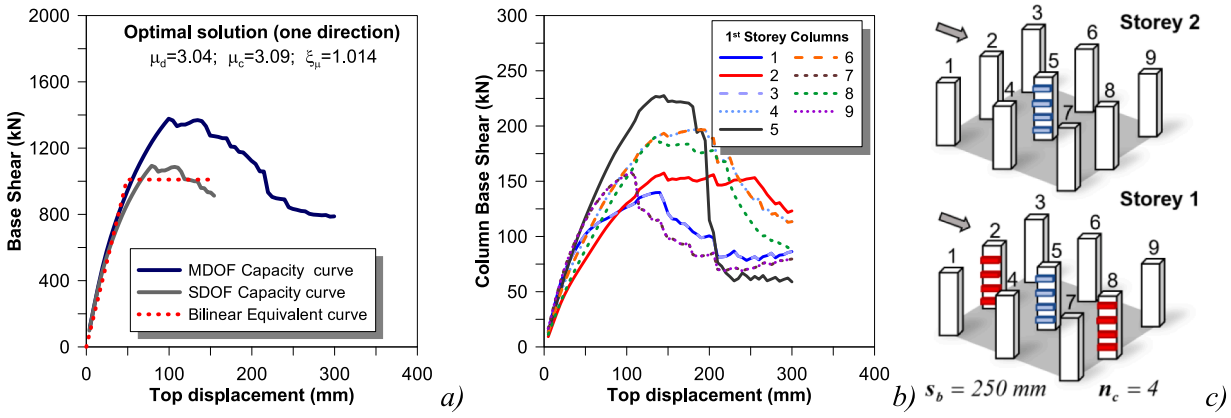

Fig. 19. Optimal solution (one direction of optimization): (a) Overall pushover capacity curves; (b) First storey columns capacity curves; (c) Retrofitting configuration at the first two stories.

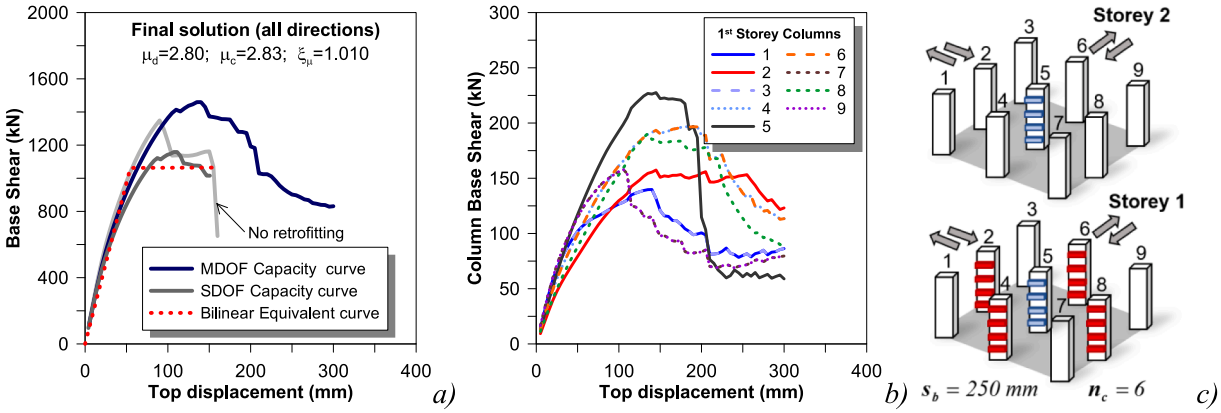

Fig. 20. Final solution (all the directions): (a) Overall pushover capacity curves; (b) First storey columns capacity curves; (c) Retrofitting configuration at the first two stories.

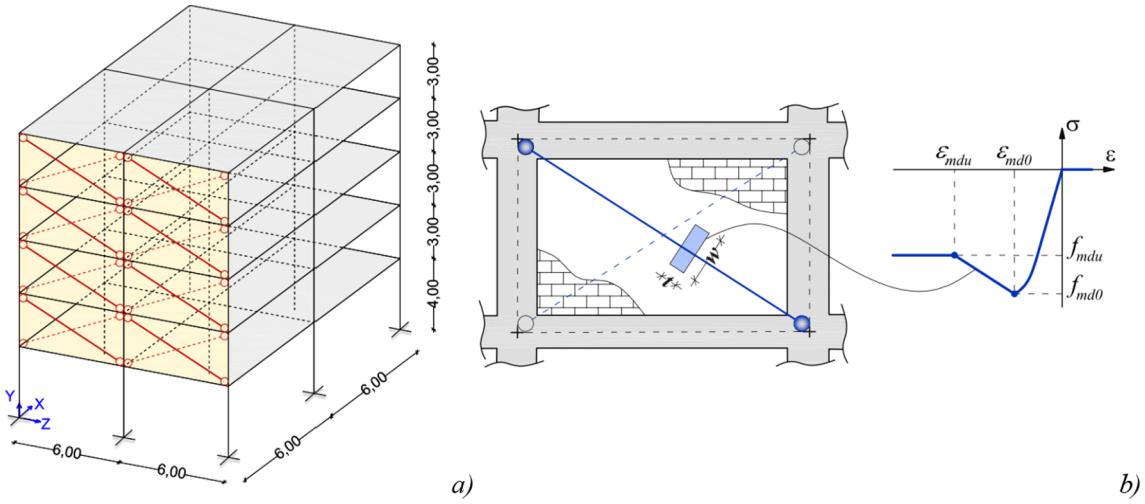

Fig. 21. Case study structure in the configuration with masonry infills: (a) Position of masonry infills; (b) Equivalent strut model.

Table 5
Geometric and mechanical details of the equivalent strut.

Infill typology	w (mm)	t (mm)	f_{md0} (MPa)	f_{mdu} (MPa)	ε_{md0} (–)	ε_{mdu} (–)
Clay hollow masonry	250	1053	1.88	0.86	0.0013	0.0073

in Z (Fig. 25). This obtained configuration is then tested with success along X direction (ξ_μ = 1.095). Finally, the cost of the intervention is 16302.59 €. Details about performances and costs can be found in Table 6. It is noteworthy observing that the cost is the same as that resulting for the bare regular frame, and this means that the proposed framework is effective in minimizing costs event in the case of structural irregularities.

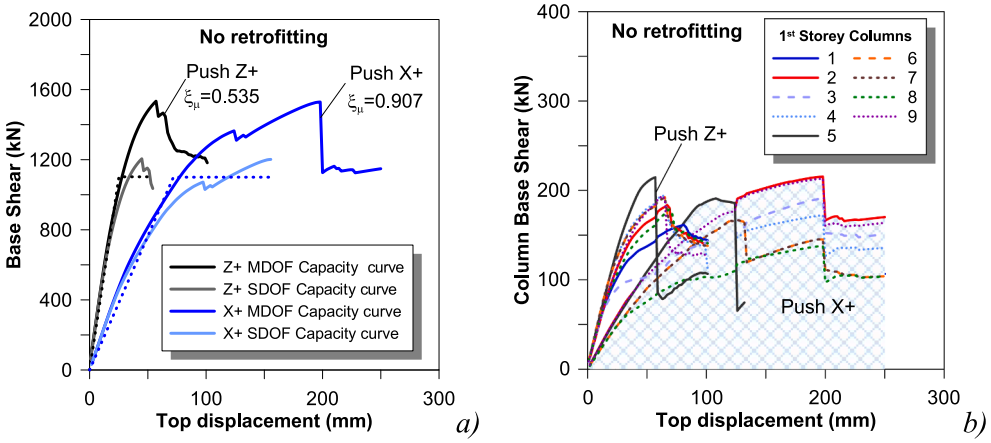

Fig. 22. Preliminary pushover cases of the non-retrofitted infilled frame along X+ and Z+ direction: (a) Overall pushover capacity curves; (b) First storey columns capacity curves.

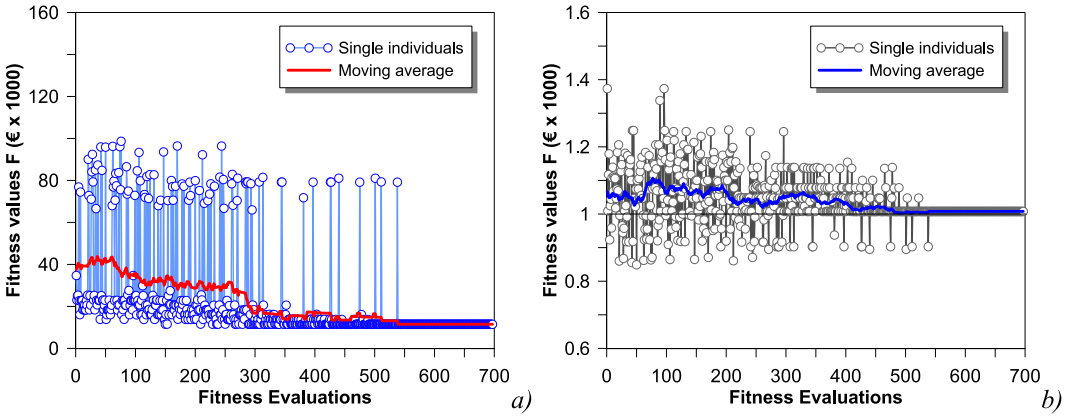

Fig. 23. Infilled frame convergence history over the fitness evaluations: (a) Cost; (b) Capacity/Demand ratio (ξ_μ).

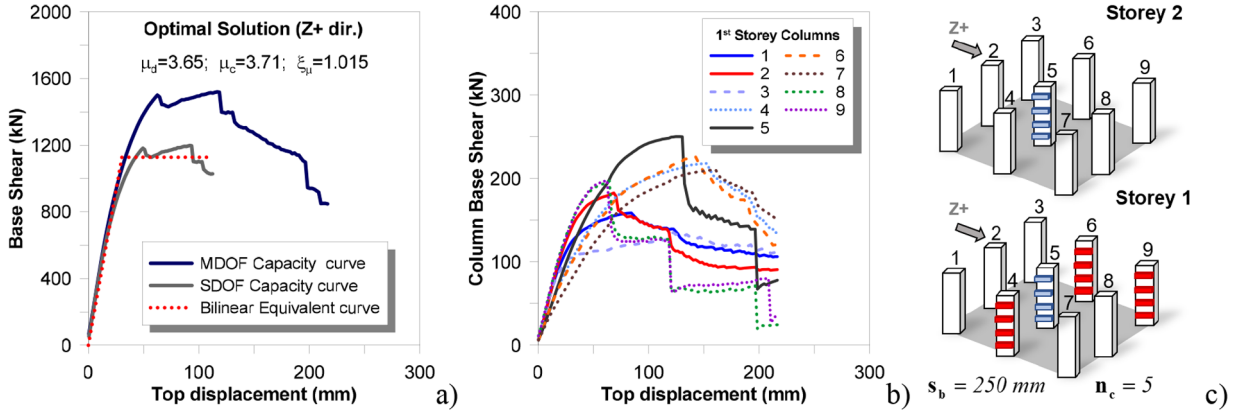

Fig. 24. Optimal solution for the infilled frame (Z+ direction): (a) Overall pushover capacity curves; (b) First storey columns capacity curves; c) Retrofitting configuration at the first two stories.

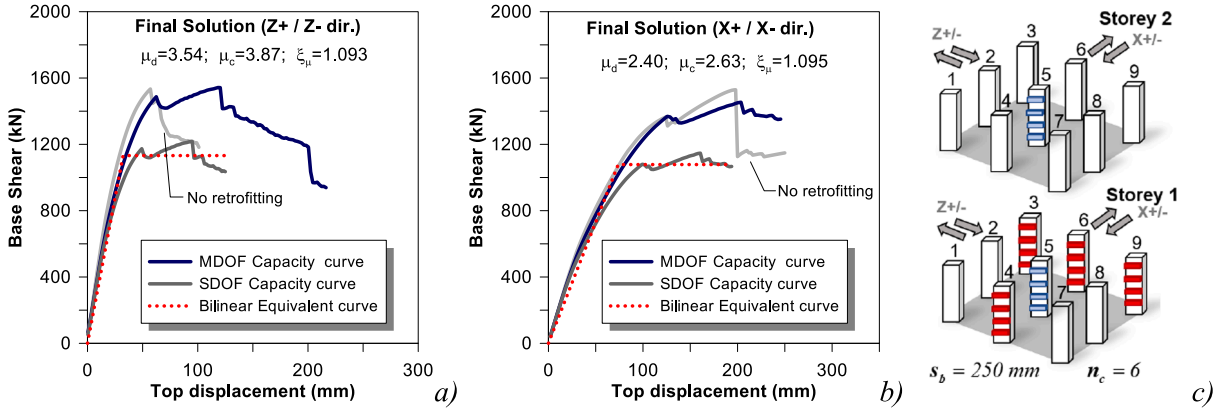

Fig. 25. Final solution (all the directions): (a) Pushover capacity curves along *Z*; (b) Pushover capacity curves along *X*; (c) Retrofitting configuration at the first two stories.

Table 6
Results of the optimization for the infilled frame.

Direction	μ_d (–)	μ_c (–)	ξ_μ (–)	s_b (mm)	n_c	C (€)	Verif. check
Z+	3.65	3.71	1.015	250	5	13585.49	Yes
Z+/−	3.54	3.87	1.093	250	5	13585.49	Yes
X+/−	2.40	2.63	1.095	250	6	16302.59	Yes

7. Conclusions

The paper presented a framework aimed at the optimization of steel jacketing retrofitting interventions of columns in reinforced concrete frame structures subjected to seismic loads. The method is associated with the adoption of nonlinear static analysis (pushover) as assessment procedure, in the framework of the N2 method. The optimization strategy used a genetic algorithm to minimize retrofitting costs operating on the number and position of reinforced columns (topological optimization) and the spacing of battens as design optimization variables. The GA was automatically connected with an interactive fiber-

section model of the structure realized with OpenSees. The feasibility of generated retrofitting solutions was controlled by the ductility capacity/demand ratio ($\xi_\mu = \mu_c/\mu_d$). The procedure was tested on a 5-storey 2-bays reinforced concrete structure. From the obtained results the following conclusion can be drawn:

- The proposed optimization framework can effectively reduce RC building retrofitting and downtime costs controlling safety levels above a specified value.
- Cost minimization associated with a reduction of the amount of steel-jacketing reinforcement is not directly connected to a reduction of safety levels, but on the contrary, the optimization allows discarding ineffective retrofitting solutions for which larger costs are associated with lower safety.
- The framework is has shown to be effective even increasing the degree of complexity of the structure, however, in the case of regular structural configurations, of configuration presenting some symmetries, the optimization can be carried out for a reduced number of directions of action of the lateral force profile in order to reduce computational effort. Retrofitting along directions not considered in the optimization can be designed based on simple suppositions of extension of the optimization results which are finally verified.
- Both for the case of simplified or full optimization, results must be interpreted as a support to the designer who will have the final decision based on his engineering judgment.
- Possible shear failure of columns and joints was not considered in the current case due to the noticeable dimensions of columns. This does not reduce the validity of the framework in general but for the cases in which the structural collapse can be conditioned by shear damage, this should be taken into account in the modelling phase or in the post-processing phase.
- The current approach has been tested on simple frame structures, however, for larger RC structures having a significant number of columns, it expected to get noticeable advantages in terms of economical and downtime costs.
- Further research and case study testing is surely needed to address, among the other aspects, the development of multiple retrofitting technique optimization algorithms and effective design optimization space restriction techniques to reduce computational effort in the cases of very complex RC building structures.

CRediT authorship contribution statement

Fabio Di Trapani: Conceptualization, Methodology, Formal analysis, Writing - review & editing, Supervision. **Marzia Malavisi:** Conceptualization, Methodology, Formal analysis. **Giuseppe Carlo Marano:** Conceptualization, Writing - review & editing, Supervision. **Antonio Pio Sberna:** Formal analysis. **Rita Greco:** Conceptualization, Writing - review & editing, Supervision.

References

[1] Campione G, Cavaleri L, Di Trapani F, Ferrotto MF. Frictional effects in structural behavior of no end-connected steel-jacketed RC columns: experimental results and new approaches to model numerical and analytical response. J Struct Eng 2017;143(8):04017070.
[2] Braga F, Gigliotti M. Analytical stress-strain relationship for concrete confined by steel stirrups and/or FRP jackets. J Struct Eng 2006;32(9):1402–16.
[3] Montuori R, Piluso V. Reinforced concrete columns strengthened with angles and battens subjected to eccentric load. Eng Struct 2009;31(2):539–50.
[4] Nagaprasad P, Sahoo DR, Rai DC. Seismic strengthening of R.C. columns using external steel cage. Earthquake Eng Struct Dyn 2009;38(14):1563–86.
[5] Tarabia AM. Strengthened of RC columns by steel angles and strips. Alexandria Eng J 2014;53(3):615–26.
[6] Adam JM, Ivorra S, Giménez E, Moragues JJ, Miguel P, Miragal C, et al. Behaviour of axially loaded RC columns strengthened by steel angles and strips. Steel Compos Struct 2007;7(5):405–19.
[7] Adam JM, Ivorra S, Pallarès FJ, Giménez E, Calderón PA. Axially loaded RC columns strengthened by steel caging: Finite element modelling. Const Build Mater 2009;23(6):2265–76.
[8] Calderón PA, Adam JM, Ivorra S, Pallarès FJ, Giménez E. Design strength of axially loaded RC columns strengthened by steel caging. Mater Des 2009;30(10):4069–80.
[9] Badalamenti V, Campione G, Mangiavillano ML. Simplified model for compressive behaviour of concrete columns strengthened with steel angles and strips. J Eng Mech 2010;136(2):230–8.
[10] Ferrotto MF, Cavaleri L, Papia M. Compressive response of substandard steel-jacketed RC columns strengthened under sustained service loads: From the local to the global behavior. Const Build Mater 2018;179:500–11.
[11] Liu M, Burns SA, Wen YK. Optimal seismic design of steel frame buildings based on life cycle cost considerations. Earthquake Eng Struct Dyn 2003;32:1313–32.
[12] Zou XK, Chan CM, Li G, Wang Q. Multiobjective optimization for performance based design of reinforced concrete frames. J Struct Eng 2007;133(10):1462–74.
[13] Greco R, Marano GC. Optimal constrained design of steel structures by differential evolutionary algorithms. Int J Optim Civil Eng 2011;3:449–74.
[14] Mitropoulou CC, Lagaros ND, Papadrakakis M. Life-cycle cost assessment of optimally designed reinforced concrete buildings under seismic actions. Reliab Eng Syst Saf 2011;96:1311–31.
[15] Akin A, Saka MP. Harmony search algorithm based optimum detailed design of reinforced concrete plane frames subject to ACI 318–05 provisions. Comput Struct 2015;147:79–95.
[16] Papavasileiou GS, Charmpis DC. Seismic design optimization of multi–storey steel–concrete composite buildings. Comp Struct 2016;170:49–61.
[17] Chaves LP, Cunha J. Design of carbon fiber reinforcement of concrete slabs using topology optimization. Con Build Mater 2014;73:688–98.
[18] Chisari C, Bedon C. Multi-objective optimization of FRP jackets for improving the seismic response of reinforced concrete frames. Am J Eng Appl Sci 2016;9(3):669–79.
[19] Seo H, Kim J, Kwon M. Optimal seismic retrofitted RC column distribution for an existing school building. Eng Struct 2018;168:399–404.
[20] Pollini N, Lavan O, Amir O. Minimum-cost optimization of nonlinear fluid viscous dampers and their supporting members for seismic retrofitting. Earthq Eng Struct Dyn 2017;46:1941–61.
[21] Braga F, Gigliotti R, Laguardia R. Intervention cost optimization of bracing systems with multiperformance criteria. Eng Struct 2019;182:185–97.
[22] Lavan O, Dargush GF. Multi-objective evolutionary seismic design with passive energy dissipation systems. J Earthq Eng 2009;13(6):758–90.
[23] Quaranta G, Lacarbonara W, Masri SF. A review on computational intelligence for identification of nonlinear dynamical systems. Nonlinear Dyn 2020;99:1709–61.
[24] Fajfar P. A nonlinear analysis method for performance-based seismic design. Earthq Spectra 2000;16:573–92.
[25] McKenna F, Fenves GL, Scott MH. Open system for earthquake engineering simulation. Berkeley: University of California; 2000.
[26] Razvi SR, Saatcioglu M. Strength and ductility of confined concrete. J Struct Eng 1992;125(3):281–98.
[27] Mander JB, Priestley MJ, Park RN. Theoretical stress-strain model for confined concrete. J Struct Eng 1988;114(8):1804–26.
[28] Eurocode 8. Design of structures for earthquake resistance—Part 1: general rules, seismic actions and rules for buildings,. Brussels: European Committee for Standardization; 2004.
[29] Campione G, Cavaleri L, Di Trapani F, Macaluso G, Scaduto G. Biaxial deformation and ductility domains for engineered rectangular RC cross-sections: a parametric study highlighting the positive roles of axial load, geometry and materials. Eng Struct 2016;107(15):116–34.
[30] Lowes LN, Mitra N, Altoontash A. A beam-column joint model for simulating the earthquake response of reinforced concrete frames PEER-2003/10 Pacific Earthquake Engineering Berkeley: Research Center, University of California; 2003.
[31] Di Trapani F, Bertagnoli G, Ferrotto MF, Gino D. Empirical equations for the direct definition of stress-strain laws for fiber-section based macro-modeling of infilled frames. J Eng Mech 2018;144(11):04018101.
[32] Di Trapani F, Malavisi M. Seismic fragility assessment of infilled frames subject to mainshock/aftershock sequences using a double incremental dynamic analysis approach. Bull Earthq Eng 2019;17(1):211–35.
[33] Di Trapani F, Giordano L, Mancini G. Progressive collapse response of reinforced concrete frame structures with masonry infills. J Eng Mech 2020;146(3):04020002.
[34] Di Trapani F, Bolis V, Basone F, Preti MG. Seismic reliability and loss assessment of RC frame structures with traditional and innovative masonry infills. Eng Struct 2020;208:110306.